NR-ART-11-2020-008076.R1-MCTS-ESI-v4.8-nov25

Electronic Supporting Information

Investigating the Influence of Block Copolymer Micelle Length on Cellular Uptake and Penetration in a Multicellular Tumor Spheroid Model

Qing Yu,[1] Megan G. Roberts,[1] Loujin Houdaihed,[2] Yang Liu,[1] Kevin Ho,[1] Gilbert Walker,[1] Christine Allen,[2] Raymond M. Reilly,[2] Ian Manners,[3] and Mitchell A. Winnik[1,4]*

[1] Department of Chemistry, University of Toronto, 80 St. George Street, Toronto, ON, M5S 1H6

[2] Leslie Dan Faculty of Pharmacy, University of Toronto, 144 College Street, Toronto, ON, M5S 3M2

[3] Department of Chemistry, University of Victoria, Victoria, British Columbia V8W 3V6, Canada

4 Department of Chemical Engineering and Applied Chemistry, University of Toronto, Toronto, ON M5S 3E2

CONTENTS **PAGE**

1. Experimental Section S2

2. Supporting Tables S8

3. Supporting Figures S10

4. References S15

EXPERIMENTAL SECTIONS

Materials

All the chemicals were purchased from Sigma-Aldrich and used as received except when mentioned specifically. The synthesis and characterization of the BCP PFS_{27}-*b*-$PAPMA_3$-*stat*-$POEGMA_{48}$ is described in Chapter 4. MTS reagent (CellTiter 96 ® AQ_{ueous} One Solution Cell Proliferation Assay) was purchased from Promega (Canada). Cell culture media DMEM, PBS buffer, and Geltrex™ Matrix were purchased from ThermoFisher Scientific.

Instrumentation

Transmission electron microscopy (TEM). All the TEM images were taken with Hitachi HT7700, at a voltage of 80 kV and a current of 10 mA in the bright-field mode. For aqueous samples, 200 mesh copper grids (Ted Pella, Inc.) with a Formvar film coated with silicon monoxide were used, whereas copper grids coated with carbon were used for imaging samples prepared from solutions in organic solvents. The number- and weight-average lengths of rod-like micelles were calculated with Eq 1, whereas the number- and weight-average diameters of spherical micelles were calculated with Eq 2,

$$L_n = \frac{\sum_{i=1}^{n} n_i L_i}{\sum_{i=1}^{n} n_i} \qquad L_w = \frac{\sum_{i=1}^{n} n_i L_i^2}{\sum_{i=1}^{n} n_i L_i} \tag{S1}$$

$$d_n = \frac{\sum_{i=1}^{n} n_i d_i}{\sum_{i=1}^{n} n_i} \qquad d_w = \frac{\sum_{i=1}^{n} n_i d_i^4}{\sum_{i=1}^{n} n_i d_i^3} \tag{S2}$$

where n_i is the number of particles with diameter d_i.

AFM topography. A spherical micelle sample in water (80 µL, 0.1 mg/mL) was drop coated onto silicon substrates (10 mm × 8 mm). The samples were covered with an inverted petri dish and dried at room temperature for at least 48 h before taking AFM measurements.

AFM height images were acquired using a Bruker Inspire™ in tapping mode with a platinum/iridium-coated tip (NanoWorld Arrow-NCPt, force constant = 42 N/m, resonance frequency = 285 kHz, tip radius < 25 nm). The data was recorded using the NanoScope v9.40 software. Images were analyzed using Gwyddion, an open source software program for SPM images (www.gwyddion.net).

AFM nanomechanical measurements. Mechanical measurements were obtained using the Inspire™ in PeakForce QNM mode with Bruker RTESPA-525 tips (force constant = 200 N/m,

resonance frequency = 525 kHz, tip radius = 8 nm). Elastic moduli were obtained by fitting the retract curve with the Derjaguin-Muller-Toporov (DMT) model[1] described in Eq. 3.

$$F_{tip} = \frac{4}{3} E^* \sqrt{Rd^3} + F_{adh} \tag{S3}$$

where F_{tip} is the load force on the tip, F_{adh} is the adhesion force, R is the tip end radius and d is the tip sample separation. Calibration was done with the relative method by imaging first on a Bruker PSFILM-12M PS calibration sample, to obtain an elastic modulus of 2.7 GPa.[2] The sample of interest was then imaged using the same parameters. The elastic modulus images were extracted using the Bruker NanoScope v9.40 software.

Cell imaging multi-mode reader. A Cytation™ 5 Cell Imaging Multi-Mode Reader (BioTek® Instruments, Inc., USA), equipped with both a digital wide field microscope and a conventional multi-mode microplate reader, was used to measure the optical density of cells for viability studies as well as to capture the images of multicellular tumor spheroids.

Flow cytometry. Cellular uptake was measured by flow cytometry, using a CytoFLEX instrument from Beckman Coulter Ltd. (USA). The flow cytometer is equipped with three lasers (488 nm, 638 nm, and 405 nm) and 13 fluorescent detectors. CytExpert and FlowJo are the software used for data analysis.

Confocal fluorescence microscopy. All the confocal fluorescence images were taken on a Zeiss LSM 700 confocal microscope in the inverted geometry with a 20X objective with 488 nm excitation and a 530/30 bandpass filter for emission. Fluorescence laser power and gain were kept constant for all the measurements.

Dynamic Light Scattering. Fixed angle dynamic light scattering (DLS) measurements were carried out using an ALV/SP-125 light scattering spectrometer equipped with an ALV-5000 multitau digital time correlator and a He−Ne laser (output power = 35 mW at λ_0 = 632.8 nm) at a scattering angle of 90°. The spherical and rod-like micelle samples were dispersed in water at a concentration of 0.02 mg/mL. All the measurements were performed at 23 °C. A cumulant analysis was employed to calculate the apparent hydrodynamic radius (z-average) and the polydispersity of the spherical and the 80 nm rod-like micelle samples.

Self-assembly of PFS_{27}-b-$PAPMA_3$-stat-$POEGMA_{48}$ micelles in solution

The preparation of rod-like micelles of lengths from 80 to 2000 nm was described previously.[3] To prepare the spherical micelle sample, the PFS_{27}-*b*-$PAPMA_3$-*stat*-$POEGMA_{48}$ BCP was dissolved in THF at 10 mg/mL and then the BCP solution (0.1 mL) was added to hot water (1.0 mL) at 90 °C. The sample was heated for 1 hour, followed by cooling to room temperature. The sample was left to age at room temperature for three days and then analyzed by TEM.

FITC conjugation of PFS_{27}-b-$PAPMA_3$-stat-$POEGMA_{48}$ micelles

Rod-like micelles prepared in ethanol were transferred to $NaHCO_3$ buffer (100 mM, pH 8.5) using the solvent exchange method described in Ref 1. Fluorescein-5-isothiocyanate (FITC) was dissolved in DMF to make a 2 mg/mL solution, and then 250 μL of this solution was added to a magnetically stirred micelle solution (2 mg/mL) in $NaHCO_3$ buffer (1 mL). The reaction was stirred in the dark overnight and then washed with water in a Amicon® Ultra-4 centrifugal filter unit (MWCO 50 kDa) for a total of six times (4000 × g, 20 min). The FITC-labeled micelles were redispersed in PBS buffer (pH 7.4) for storage and further analysis.

Cell lines

The two human breast cancer cell lines MDA-MB-231, MDA-MB-436 were purchased from the American Type Culture Collection (Manassas, VA). The cells were cultured in DMEM/F-12 media supplemented with 1 % penicillin-streptomycin (P/S) and 10% fetal bovine serum (FBS) at 37 °C and 5 % CO_2.

Cell monolayer viability assays

The viability of the two cell lines incubated with the BCP micelles was determined using the MTS cell proliferation colorimetric assay. The MTS solution was prepared by mixing 50 mg of MTS reagent and 5.25 mg of phenazine ethosulfate in 25 mL PBS buffer. Cells were seeded at a density of 2000 cells per well in 96-well plates (Nunc 96-Well Flat Bottom, ThermoFisher Scientific), followed by incubation at 37 °C and 5 % CO_2 for 24 h. Cells were then treated with FITC-labeled micelles of different lengths from 80 to 2000 nm. The micelle solutions were used in ten 1:10 serial dilutions, starting from 0.1 mg/mL. After 24 h, 20 μL MTS reagent solution was added to each well, and the cell viability was measured by UV/Vis absorption at 490 nm using a plate reader (Cytation 5 imaging reader, BioTek®).

Cellular uptake

For micelle uptake studies, MDA-MB-231 and MDA-MB-436 cells were seeded at a density of 1 x 10^5 cells per well in 24-well plates and incubated overnight to allow for cell attachment. After the incubation, cell culture media was removed and replaced with 1 mL of FITC-labelled micelle solution (0.1 mg/mL in fresh media). Cells were incubated for 24 h in the dark. Subsequently, the cell supernatant was removed, and the cells were washed three times with PBS buffer by centrifugation (1500 rpm, 3 min). Cells were re-suspended in 0.5 mL PBS and analyzed on a flow cytometer (CytoFLEX). The FITC channel was selected to detect the fluorescence intensity from 5000 cells for each experiment. Cells that were incubated with culture media in the absence of FITC-labelled micelles were used as a negative control to measure their autofluorescence.

Multicellular tumor spheroid preparation

Multicellular tumor spheroids (MCTS) were prepared using a liquid overlay method in ultra-low adhesive 96U bottom plates (Nunclon™ Sphera™ Microplates, ThermoFisher Scientific, Denmark). MDA-MB-436 cells were seeded at a concentration of 5000 cells/well in 100 μL cell culture media. MDA-MB-231 cells were seeded at a concentration of 1000 cells/well in 100 μL culture media containing 2% (v/v) Geltrex™ Matrix (Gibco™). Centrifugation (400 RCF, 10 min) was used to facilitate the formation of MDA-MB-231 MCTS.[4] Both MDA-MB-436 and MDA-MB-231 MCTSs were incubated in complete growth media for four days at 37 °C in 5% CO_2. Every other day, 50 μL of the culture media was removed and replaced by fresh media. The spheroids reached a diameter of ~500 μm on Day 4.

Cell packing density in MCTS

To determine the cell packing density in MDA-MB-231 and MDA-MB-436 MCTSs, a group of 12 MCTSs were combined, and trypsinization was employed to dissociate the cells from the spheroids. The total number of cells was counted using a Bio-Rad TC automated cell counter and then divided by 12 to obtain the average number of cells per MCTS. Cell packing density was calculated by dividing the number of cells per MCTS by the volume of MCTS.[5] The volume of MCTS was calculated from the MCTS diameter measured by a Cytation 5 imaging reader, BioTek®.

Micelle penetration into MCTS

MCTS reached a diameter of approximately 500 μm on Day 4. To study the micelle penetration into MCTS, half of the cell culture media was removed and then replaced by 50 μL of micelle solution. The final micelle concentration was 0.1 mg/mL in each well. After 24 h incubation in the dark, each MCTS was washed 5 times with PBS buffer and then transferred to a Nunc™ glass bottom dish (ThermoFisher) for confocal fluorescence microscopy measurements.

Methodology for interpreting micelle penetration into MCTS

The penetration of micelles into MCTS was examined by confocal microscopy (Zeiss LSM 700) using a protocol established by the Allen group.[6, 7] The images were captured with a 20X objective and a FITC filter (λ_{ex} 488 nm, λ_{em} 580 nm). The 488 nm line of an Argon/2 (GFP/FITC) laser was used and the laser power was set at 0.5 % for live cell imaging. Identical microscopy settings were used when imaging MCTSs from the same cell line to ensure standardized comparison between different micelles. As illustrated in Figure S6a, optical slices were taken at different depths (30, 50, 60, and 90 μm) from the bottom surface of each spheroid, and images showing MCTS cross-sections were captured accordingly. In this study, we adopted the approach used by Eetezadi et al.,[5] in which penetration of micelles into MCTS was assessed using slices taken at 30, 60, and 90 μm depths, while images at 50 μm were used to determine the micelle accumulation.[5] On the image of each optical slide, the MCTS cross-section was divided into three equally spaced concentric regions as shown in Figure S6b, namely the periphery (P, green), the intermediate (I, yellow), and the core (C, red) regions. Note that the core here refers to the central section in the confocal images acquired at different depth in the MCTS, not the core of the spheroid. The laser equipped in the confocal microscope has a limited penetration depth of ~100 μm, and thus it cannot take the optical slice at the center of a ~500 μm diameter MCTS. To assess the penetration of different $^{FITC}PFS_{27}$-*b*-$PAPMA_3$-*stat*-$POEGMA_{48}$ micelles in MCTS, the fluorescence intensity per unit area from the three regions was analyzed by ImageJ (Figure S6) and comparisons between these three regions were performed with SPSS software. Statistical significance was set at $p < 0.05$.

Statistical analysis

In the cell studies, all the data are presented as the mean of at least three independently performed experiments ± SD. For comparison between two groups, 2-tailed independent-sample

t-tests were carried out. For comparison between more than two groups, one-way ANOVA was performed with subsequent posthoc analyses with a Bonferroni correction. Statistical significance was defined as $p < 0.05$. All the statistical tests were performed using IBM SPSS statistical software (SPSS Inc.).

ADDITIONAL RESULTS AND DISCUSSION

Spherical PFS_{27}-b-$PAPMA_3$-stat-$POEGMA_{48}$ micelles

To prepare a sample of spherical micelles, we took a solution of PFS_{27}-*b*-$PAPMA_3$-*stat*-$POEGMA_{48}$ BCP in THF and added it to hot water. The mixture was heated at 90 °C for 1 hour and then rapidly cooled to room temperature to yield spherical micelles. The exposure of the hydrophobic PFS core to the polar aqueous medium created a high interfacial energy, driving the rapid formation of spherical micelles on a much faster time scale than that needed for PFS crystallization.[8, 9] A TEM image of these spherical micelles is presented in **Error! Reference source not found.**a, showing a number average core diameter (d_n) of 72 nm. The core radius was found to be longer than the extended length of the PFS block, which is 0.7 nm × 27 = 19 nm.[10] This result suggests that these spherical aggregates are likely to be compound micelles.[11, 12] The hydrodynamic size of the spherical micelle sample in water was measured by DLS at a 90° scattering angle. From a cumulant analysis, the spherical micelles have a z-average R_h = 41 nm (PDI = 0.168).

A corresponding tapping-mode AFM image is presented in Figure S1a,b. The mean height of 30 nm suggests that some deformation occurred as the sample dried on the grid. A corresponding image taken in the QNM (Quantitative Nanoscale Mechanical) mode (Figure S1c,d) showed a core-shell structure with a rigid PFS core (Young's modulus E= 7.30 ± 0.60 GPa) and a somewhat softer shell (E = 1.22 ± 0.13 GPa) that is likely associated with a POEGMA-rich corona. The stiffness of the PFS core is consistent with the idea that the amorphous PFS core is in a glassy state (T_g = 33 °C)[13] at room temperature.

Toxicity PFS_{27}-b-$PAPMA_3$-stat-$POEGMA_{48}$ micelles

The potential toxicity of the micelle samples was examined by the MTS cell viability assay using two human breast cancer cell lines (MDA-MB-231 and MDA-MB-436). Raw data showing the % cell viability as a function of micelle concentration are in Figure S3. The results from both

cell lines showed that the micelles were non-toxic to cells up to a concentration of 0.1 mg/mL. The cell viability was not affected by the length of the rod-like micelles. Since the micelles are non-toxic to breast cancer cells, then they may be suitable delivery vehicles to insert cytotoxic drugs into tumor cells.

SUPPORTING TABLES

Table S1 Summary of cellular uptake data from MDA-MB-436 cells

	% Uptake					Median fluorescent intensity				
Length (nm)	**1**	**2**	**3**	**average**	**SD**	**1**	**2**	**3**	**average**	**SD**
80	98.9	98.0	98.5	98.4	0.48	17830	17013	13964	16269	2037
200	97.7	95.5	97.4	96.8	1.20	11787	11283	11786	11619	290
500	94.6	93.6	93.7	93.9	0.54	9724	12823	9482	10676	1863
1000	93.1	89.7	92.9	91.9	1.89	7970	8223	8029	8074	132
2000	77.3	73.1	70.4	73.6	3.48	4843	5150	4319	4771	420
spherical	35.4	27.9	29.6	31.0	3.95	2864	3009	2551	2808	234
negative	n/a					826	815	924	855	60

Table S2 Summary of cellular uptake data from MDA-MB-231 cells

	% Uptake					Median fluorescent intensity				
Length (nm)	**1**	**2**	**3**	**average**	**SD**	**1**	**2**	**3**	**average**	**SD**
80	34.0	34.7	33.6	34.1	0.59	18320	18810	17890	18340	460
200	15.6	16.3	15.7	15.9	0.41	12177	12394	12357	12309	116
500	32.2	35.9	31.4	33.2	2.36	15769	16723	15358	15950	700
1000	22.7	26.7	23.3	24.2	2.17	13898	13776	14062	13912	144
2000	19.4	30.7	30.2	26.8	6.38	14021	16144	15906	15357	1163
spherical	9.9	12.9	14.9	12.6	2.55	10733	12763	10670	11388	1191
negative	n/a					7050	6669	6788	6836	195

Table S3 Fluorescence intensity per area of $^{FITC}PFS_{27}$-*b*-$PAPMA_3$-*stat*-$POEGMA_{48}$ micelles at selected depths from the surface of MDA-MB-436 MCTSs

MDA-MB-436		sph		80 nm		200 nm		500 nm		1000 nm		2000 nm	
30 µm	P	5.92	± 0.96	10.02	± 2.02	10.96	± 2.66	10.06	± 1.79	6.78	± 1.66	6.83	± 0.68
	I	6.12	± 0.40	9.60	± 1.66	10.91	± 1.76	10.17	± 0.94	6.64	± 1.95	7.03	± 0.48
	C	5.67	± 1.49	8.87	± 1.01	10.13	± 1.34	9.34	± 0.57	5.55	± 0.47	7.84	± 0.18
50 µm	P	3.77	± 0.28	7.87	± 0.25	4.05	± 1.15	4.79	± 0.57	3.95	± 0.44	2.87	± 0.33
	I	2.93	± 0.53	6.79	± 2.11	4.41	± 2.93	2.82	± 0.72	1.75	± 0.67	1.64	± 0.19
	C	2.49	± 0.54	6.59	± 1.86	3.87	± 2.49	2.70	± 0.86	0.89	± 0.55	1.81	± 0.15
60 µm	P	2.98	± 0.49	6.07	± 0.89	5.23	± 2.19	3.22	± 0.78	2.90	± 0.42	2.50	± 0.32
	I	1.83	± 0.15	4.69	± 2.20	3.77	± 1.67	1.60	± 0.26	1.65	± 0.52	0.99	± 0.36
	C	1.58	± 0.28	5.23	± 2.19	3.65	± 1.86	1.60	± 0.20	0.69	± 0.58	1.16	± 0.42
90 µm	P	1.59	± 0.33	1.94	± 0.52	2.39	± 0.72	2.69	± 1.04	1.04	± 0.45	0.82	± 0.13
	I	0.83	± 0.08	1.11	± 0.36	1.55	± 1.07	1.22	± 0.45	0.42	± 0.20	0.45	± 0.09
	C	0.66	± 0.26	1.13	± 0.33	1.37	± 0.60	1.06	± 0.48	0.32	± 0.08	0.51	± 0.11

SUPPORTING FIGURES

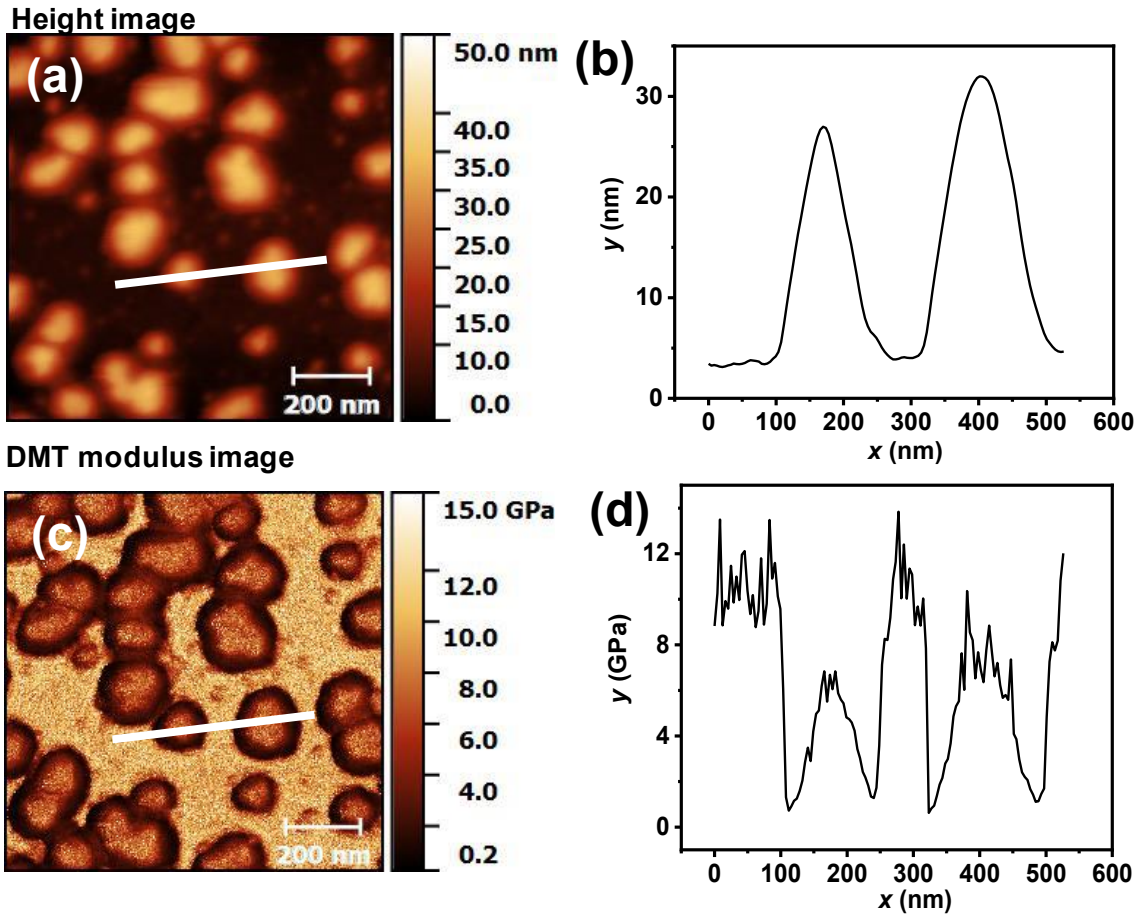

Figure S1 The maps of the topography and elastic DMT modulus obtained in tapping and PeakForce QNM imaging modes. (a) height and (b) the corresponding line profile; (c) DMT modulus and (d) the corresponding line profile.

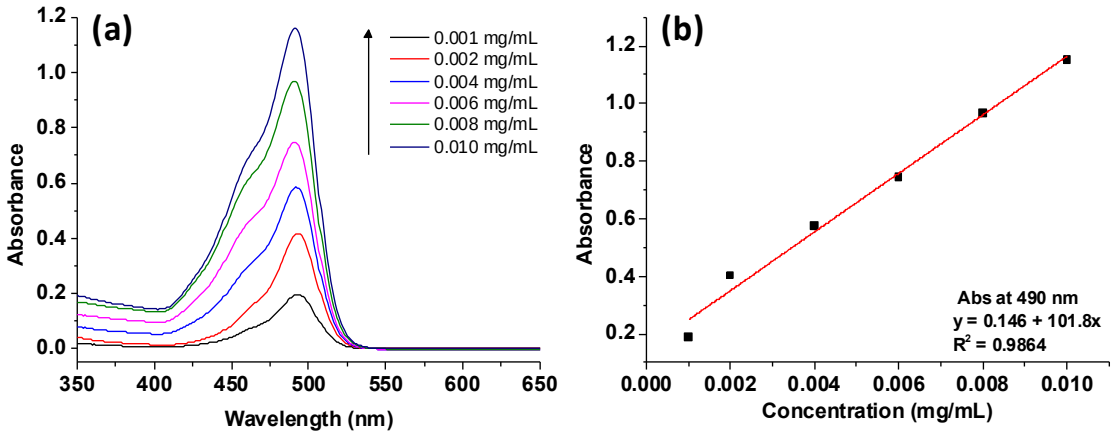

Figure S2 (a) Absorption spectra of FITC in PBS buffer (pH 7.4) at different concentrations. (b) Calibration curve of FITC, plotted as absorbance at 490 nm vs. concentration.

MDA-MB-231

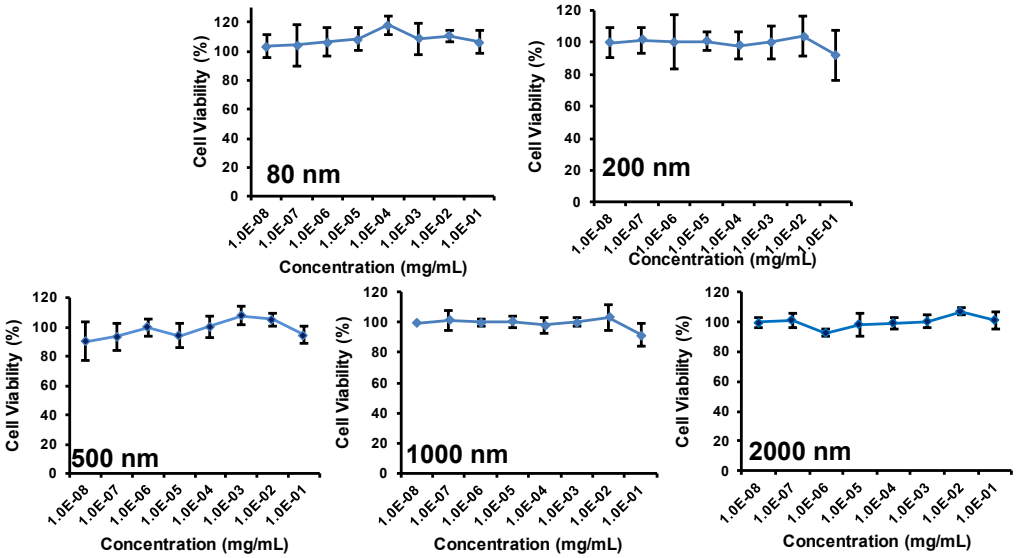

MDA-MB-436

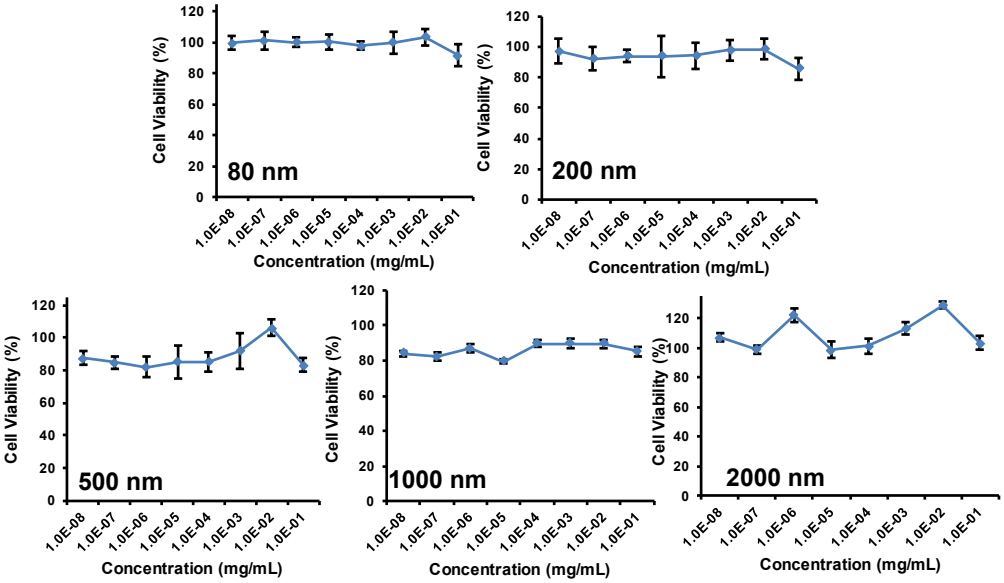

Figure S3 Cell viability MTS assay using (top) MDA-MB-231 cells and (bottom) MDA-MB-436 cells treated with increasing concentrations of rod-like $^{FITC}PFS_{27}$-*b*-$PAPMA_3$-*stat*-$POEGMA_{48}$ micelles from 10^{-8} to 10^{-1} mg/mL. Five rod-like micelle samples of different lengths (80, 200, 500, 1000, and 2000 nm) were tested and showed non-toxic to cells up to 0.1 mg/mL.

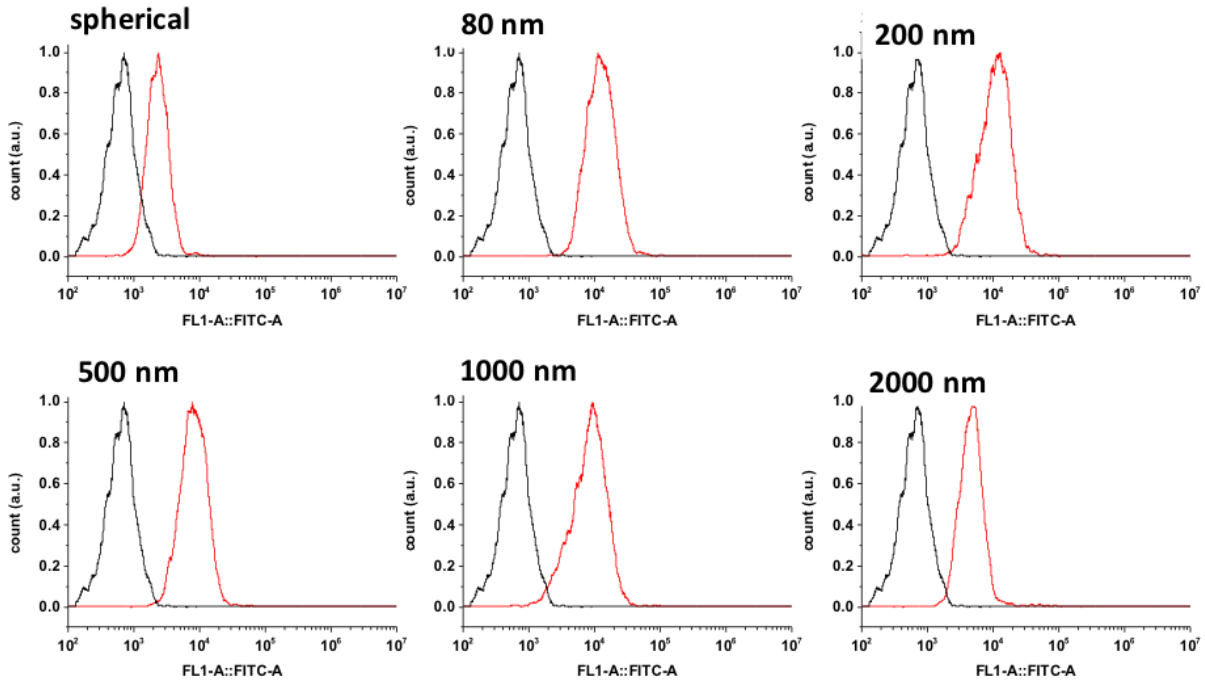

Figure S4 Flow cytometry analysis of MDA-MB-436 cells after incubating with 0.1 mg/mL of $^{FITC}PFS_{27}$-*b*-$PAPMA_3$-*stat*-$POEGMA_{48}$ micelles for 24 h. Cellular uptake experiments were conducted on spherical micelles of diameter 72 nm and rod-like micelles with lengths of 80, 200, 500, 1000, and 2000 nm.

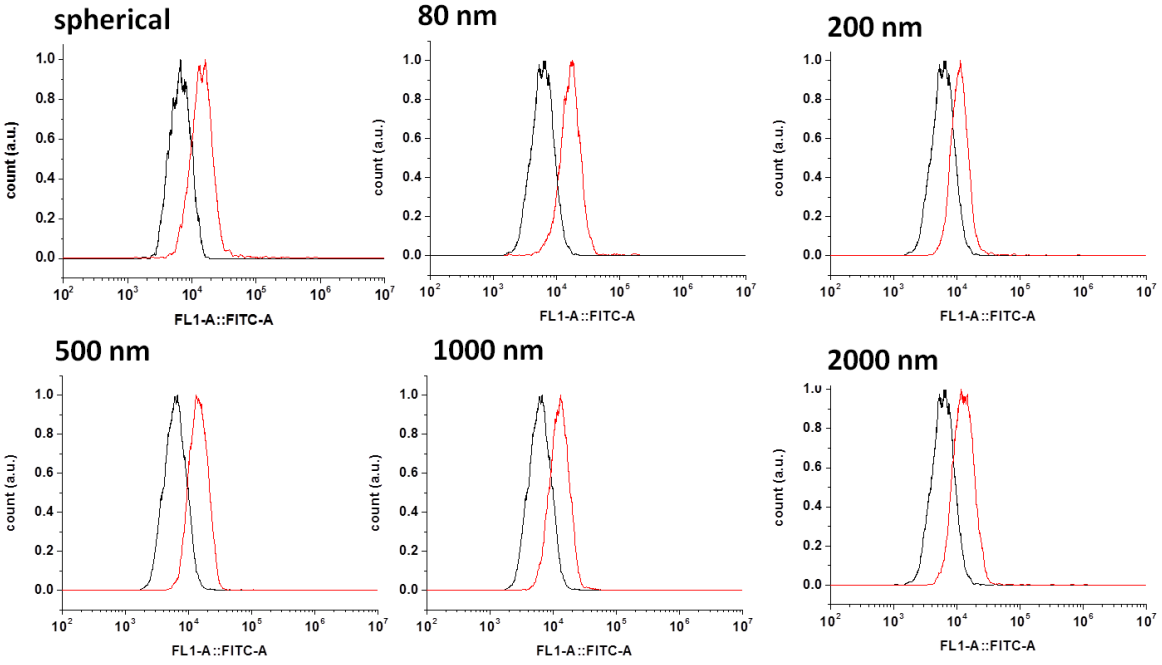

Figure S5 Flow cytometry analysis of MDA-MB-231 cell line after incubating with 0.1 mg/mL of $^{FITC}PFS_{27}$-*b*-$PAPMA_3$-*stat*-$POEGMA_{48}$ micelles for 24 h. Cellular uptake experiments were conducted on spherical micelles of diameter 72 nm and rod-like micelles with lengths of 80, 200, 500, 1000, and 2000 nm.

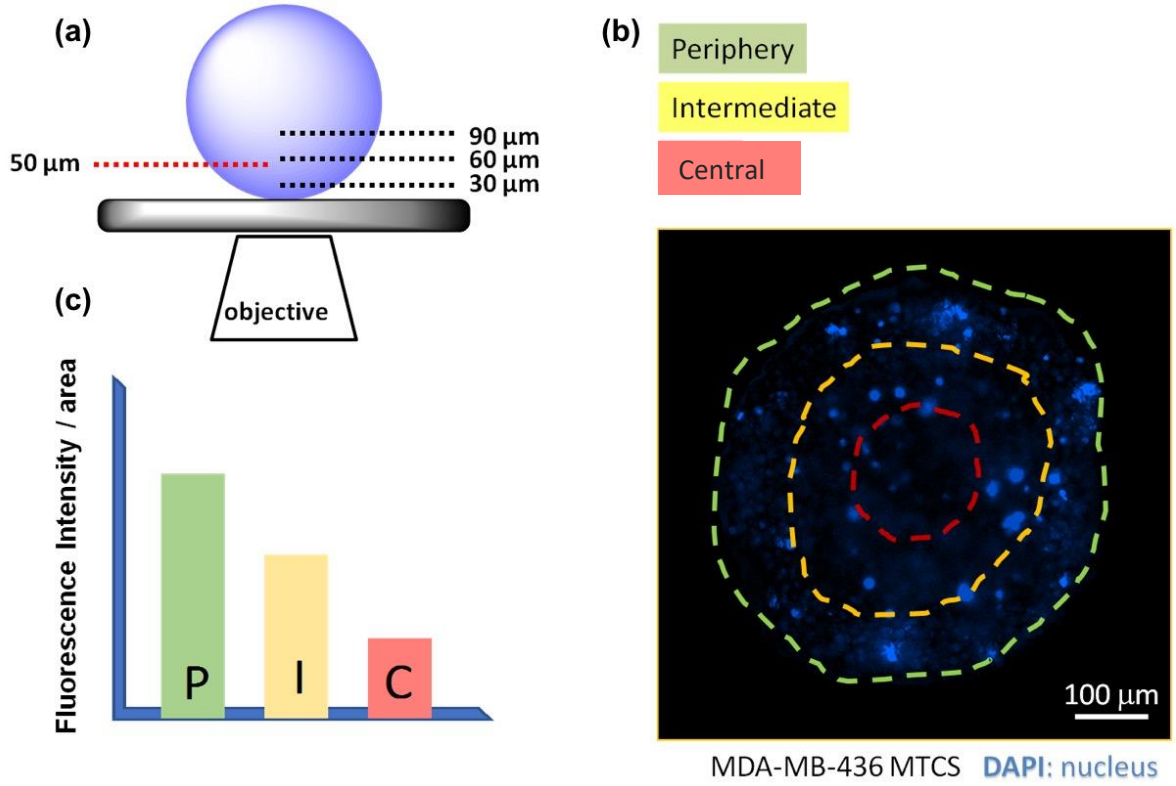

Figure S6 Interpretation of confocal images. (a) A scheme showing the microscope set-up and positions to obtain optical slices in MCTS. (b) Cross-section of MCTS, at different depth from the spheroid surface, was equally divided to three concentric regions (periphery, intermediate, and core) and color coded. (c) The fluorescence intensity per unit area was determined for P, I, and C regions by ImageJ software.

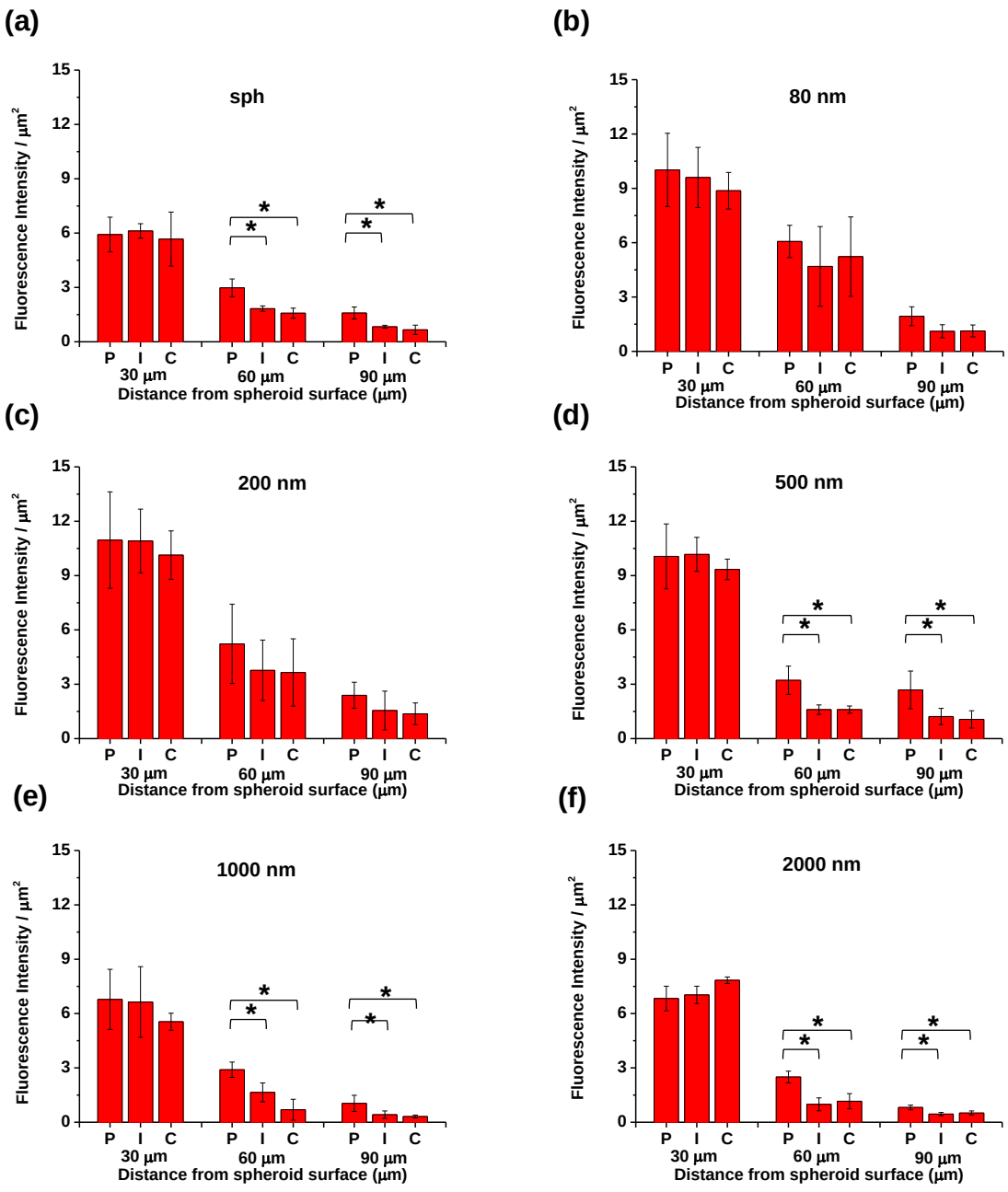

Figure S7 Assessment of $^{FITC}PFS_{27}$-*b*-$PAPMA_3$-*stat*-$POEGMA_{48}$ micelle penetration into MDA-MB-436 MCTSs. (a) Spherical micelles of d_n = 72 nm and rod-like micelles of L = (b) 80 nm, (c) 200 nm, (d) 500 nm, (e) 1000 nm, and (f) 2000 nm were incubated with the MCTSs under the identical conditions at 0.1 mg/mL To quantify micelle penetration, the total fluorescence intensity per unit area was calculated for the periphery (P), intermediate (I), and core (C) region of each MCTS, using the confocal images in **Error! Reference source not found.**. Data points represent mean ± standard deviation in each area, n = 3 MCTSs. Statistically significant differences between each region are denoted by (*), and in all cases p < 0.05.

REFERENCES

1. B. V. Derjaguin, V. M. Muller and Y. P. Toporov, *J. Colloid Interface Sci.*, 1975, **53**, 314-326.
2. M. E. Dokukin and I. Sokolov, *Langmuir*, 2012, **28**, 16060-16071.
3. Q. Yu, M. G. Roberts, S. Pearce, A. M. Oliver, H. Zhou, C. Allen, I. Manners and M. A. Winnik, *Macromolecules*, 2019, *52*(14), 5231-5245.
4. C. Dubois, R. Dufour, P. Daumar, C. Aubel, C. Szczepaniak, C. Blavignac, E. Mounetou, F. Penault-Llorca and M. Bamdad, *Oncotarget*, 2017, **8**, 95316-95331.
5. S. Eetezadi, R. De Souza, M. Vythilingam, R. Lessa Cataldi and C. Allen, *Mol Pharm*, 2015, **12**, 3973-3985.
6. A. S. Mikhail, S. Eetezadi, S. N. Ekdawi, J. Stewart and C. Allen, *Int J Pharm*, 2014, **464**, 168-177.
7. A. S. Mikhail, S. Eetezadi and C. Allen, *PLoS One*, 2013, **8**, e62630.
8. X. Wang, M. A. Winnik and I. Manners, *Macromolecules*, 2005, **38**, 1928-1935.
9. R. L. Hailes, A. M. Oliver, J. Gwyther, G. R. Whittell and I. Manners, *Chem Soc Rev*, 2016, **45**, 5358-5407.
10. G. Guerin, P. Rupar, G. Molev, I. Manners, H. Jinnai and M. A. Winnik, *Macromolecules*, 2016, **49**, 7004-7014.
11. W. Lin, C. Zheng, X. Wan, D. Liang and Q. Zhou, *Macromolecules*, 2010, **43**, 5405-5410.
12. L. Zhang and A. Eisenberg, *Journal of the American Chemical Society*, 1996, **118**, 3168-3181.
13. R. G. H. Lammertink, M. A. Hempenius, I. Manners and G. J. Vancso, *Macromolecules*, 1998, **31**, 795-800.